

Oxidation of arsenopyrite (FeAsS) in acid Part II: Stoichiometry and reaction scheme

P. G. FERNANDEZ

School of Applied Chemistry, Curtin University, Bentley, Australia, 6102

H. G. LINGE*, M. J. WILLING

CSIRO DMP, Curtin University, Bentley, Australia, 6102

Received 19 June 1995; revised 24 November 1995

The electrochemical oxidation of arsenopyrite (FeAsS) in 0.01 M chloride solution at pH 2 has been investigated and the effect of electrode potential, temperature and arsenopyrite mineral composition on the reaction stoichiometry studied. Iron, arsenic and sulfur products were formed in the ratio 1:1:1, for all conditions for arsenic deficient and stoichiometric arsenopyrite. Product speciation was dependent on temperature and potential, but not on arsenopyrite composition. At 25 °C, Fe(II), Fe(III), As(III), As(V), S, SO_4^{2-} and S(x) (which could be a polythionate such as tetrathionate or pentathionate) were formed and $\sim 9e^-$ produced per mol of arsenopyrite oxidized. At 75 °C, practically no S(x) was formed and $7.5e^-$ produced per mol of arsenopyrite oxidized. A qualitative reaction scheme, based on the decomposition of thiosulfate to polythionate in the presence of As(III), is outlined.

1. Introduction

This paper extends the previous work [1] on the electrochemical reactivity of arsenopyrite in acid. The chemistry of arsenopyrite oxidation has been studied by electrochemical oxidation of mineral electrodes between 0.7–1 V vs SHE in dilute chloride solution at pH 2, relevant to low temperature preoxidation of refractory gold containing arsenopyrite ores by slurry oxidation in saline plant liquors [2, 3]. Proven analytical techniques have been used to delineate the speciation of reaction products at 25 and 75 °C for stoichiometric and arsenic-deficient arsenopyrite.

Previous studies of arsenopyrite oxidation at atmospheric pressure [4–13] have not attempted to identify specifically the species generated in the reaction. Instead, calculated E_h /pH diagrams, infra red and XPS spectra or interpretation of voltammograms were used to postulate reaction products. A detailed study of the oxidation of arsenopyrite in pressurized sulfuric acid solutions between 130–180 °C has been carried out by Papangelakis and Demopoulos [14, 15]. The oxidation stoichiometry with respect to iron and arsenic was congruent (i.e., 1:1). Iron was released as Fe(II) but was slowly oxidized to Fe(III) by oxygen in solution. 85–90% of the dissolved arsenic was found as As(V). Sulfur was released predominantly as SO_4^{2-} , though small amounts of S ($\leq 20\%$) were also formed. It was postulated that the oxidation process proceeds via two competing parallel

pathways, for the formation of SO_4^{2-} and S. However, the sulfur pathway was considered to be self inhibiting and the reactions listed do not allow prediction for the speciation of reaction products.

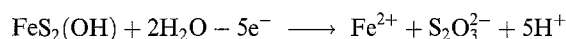
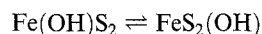
There are numerous studies of the aqueous oxidation of mineral sulfides other than arsenopyrite in acid solution (e.g., [16–21]). Most investigators consider that it is the sulfide sublattice which is oxidized in the reaction. The metal constituents are treated as cations which are hydrated once the sulfide sublattice has been destroyed by oxidation. In acid, S and SO_4^{2-} are the two most common sulfur reaction products. Most sulfides form S with little SO_4^{2-} but pyrite oxidation produces predominantly SO_4^{2-} . The SO_4^{2-} yield changes from 75–100% as the oxidation potential is increased from 1–1.5 V but this fact could not be explained [19]. It has been shown [22] that the SO_4^{2-} oxygen originates from water, and Meyer [18] proposed that SO_4^{2-} is formed from intermediates such as thiosulfate, $\text{S}_2\text{O}_3^{2-}$.

Dutrizac [21] suggested that S is formed for all conditions via dissolved H_2S . Alternatively, if sulfide predominates in forming the bonding electronic states in the lattice, oxidation by direct charge exchange involving these states could directly lead to the formation of S at the surface via metal deficient sulfide surface phases [17] which have been identified on many metal sulfides by XPS spectroscopy (e.g., [23]).

More recently, semiconductor concepts have been invoked to account for the sulfur speciation in sulfide oxidation (e.g., [24, 25]). For pyrite, the upper edge of the valence band consists primarily of a nonbonding orbital derived from Fe; oxidation of the sulfide by

* Author for correspondence at PO Box 482, Kalamunda, Australia, 6076.

injection of a hole into this orbital does not break the lattice but is available to slowly split water. The reaction pathway suggested is as follows [25]:



In acid, the surface thiosulfate slowly decomposes to form S and bisulfite HSO_3^- . At pH 2, thiosulfate has been detected in solution. This ion and bisulfite can be readily oxidized to SO_4^{2-} on an electrode. This mechanism can account qualitatively for the experimental potential dependence of SO_4^{2-} formation if the first step in the scheme is rate determining. As the electronic structure of arsenopyrite is only partially understood [26] it is difficult to assess the relevance of semiconductor concepts to arsenopyrite oxidation. In [1], we found no significant difference in the reactivities of stoichiometric, n- and p-type arsenopyrite but this fact need not eliminate the above mechanistic pathway if the upper edge of the valence band in arsenopyrite is little affected by the small variations in composition typical for natural arsenopyrite [26, 27].

2. Experimental details

Experimental procedures used to oxidize arsenopyrite electrochemically between 0.7–1 V vs SHE were as described [1]. The Pt counter electrode was separated from the bulk solution with a fritted glass disc to prevent contact with the reaction products. Charge passed was measured with an Amel digital integrator (type 731) connected in series with the counter electrode. Most tests used arsenic deficient arsenopyrite $\text{Fe}_{1.00}\text{As}_{0.92}\text{S}_{1.00}$ from Santa Eulalia (Mexico) because this material had the largest surface area in our samples [27], improving the analysis accuracy of pregnant solutions. A few tests were made with stoichiometric arsenopyrite from Greenbushes (Australia) to confirm lack of influence from arsenopyrite composition [1]. The background electrolyte was 0.01 M KCl at pH 2 to mimic acidified saline plant liquor but minimize the effect of dissolved salt on solution analysis [27].

Samples of cell solution were taken at various stages and at the end of an experiment and the reaction products analysed. The analysis techniques used are well known but were adapted for the present experimental conditions as described in detail in [27] and references therein. Analysis uncertainty was ± 5 –10%, or less. Total dissolved iron, arsenic and sulfur was analysed simultaneously by inductively coupled plasma-atomic emission spectrometry (ICP–AES) at 259.9, 193.8 and 180.7 nm, respectively, with an Applied Research Laboratories A250A spectrometer. Dissolved iron(II) was analysed as the 2,2-dipyridyl complex at 520 nm with a Varian DMS 80 dual beam spectrophotometer. Dissolved arsenate and sulfur anions were determined simultaneously by ion chromatography (IC) using a pH 9.5 sodium bicarbonate/carbonate eluent and a conductivity

Table 1. Effect of preoxidation of dissolved arsenopyrite solutions on IC analysis and a comparison to ICP–AES analysis of the same solutions

Treatment adopted	SO_4^{2-} result by IC /ppm	Dissolved S by ICP–AES /ppm
No preoxidation	9.5	16.0
Preoxidation	15.4	16.0

detector (Dionex 2110i ion chromatograph). Prior to IC analysis, all iron was removed from solution with a Bond Elut SCX cation exchange resin (Analytichem International) as iron interfered in the arsenate analysis. At the end of an experiment, the solid reaction products were scraped from the electrode surface and analysed by dispersive X-ray analysis (SEM/EDX) and X-ray diffraction (XRD). S in the deposit was dissolved in carbon disulfide for determination from the weight of the residue after evaporation (sensitivity 0.2 mg).

The IC and ICP–AES analyses for SO_4^{2-} were shown to be concordant within $\pm 5\%$ using synthetic SO_4^{2-} solutions. A test solution containing dissolved arsenopyrite was split and one portion oxidized with H_2O_2 prior to analysis with IC and ICP–AES. Preoxidation had no influence on the ICP–AES analysis, confirming that this measurement determined total dissolved sulfur. However, the IC analysis was affected, for example, as shown in Table 1.

The IC result for the untreated solution was lower than for preoxidized solution, for which it corresponded to the ICP–AES result; demonstrating the presence of a soluble sulfur species with a lower oxidation state than S(vi) in the original solution. IC showed that sulfite was not present in the original solution and the unknown species has been termed S(x), where $x < 6$ denotes the oxidation state. The likely identity of S(x) will be discussed later below and the amount produced was calculated thus: $\text{S}(x) = \text{total dissolved sulfur (ICP–AES)} - \text{sulfate (IC)}$.

3. Results and discussion

3.1. Oxidation stoichiometry

Table 2 summarizes the oxidation stoichiometry for arsenic deficient arsenopyrite at three potentials at 25 °C based on final values for each element for duplicate experiments at each potential. The uncertainties for Fe and As are $\pm 2\%$ and $\pm 5\%$, respectively. In the case of the sulfur stoichiometry, there are two forms of sulfur to consider. S is formed on the electrode surface and dissolved sulfur is formed in solution (analytical uncertainty $\pm 5\%$). The percentage uncertainties in analyses for S are not fixed in each case and depend on the mass of material collected e.g., at 0.74 V for the first value it was 25 μmol or 0.8 ± 0.2 mg, which equates to an uncertainty of $\pm 24\%$. This larger uncertainty for S increased the uncertainty in the total sulfur released, in this case to $\pm 12\%$.

Table 2. Oxidation of arsenic deficient arsenopyrite ($\text{FeAs}_{0.92}\text{S}$) at different potentials (vs SHE) and 25 °C in 0.01 M KCl at pH 2. Repeated tests used different electrodes

Potential <i>V</i> vs SHE	Total dissolved Fe/ μmol	Total dissolved As/ μmol	Total dissolved S/ μmol	Total elemental S/ μmol	Oxidation stoichiometry
0.74	74	72	41	25	$\text{Fe}_{1.00}\text{As}_{1.00\pm 0.05}\text{S}_{0.9\pm 0.1}$
	92	90	49	34	$\text{Fe}_{1.00}\text{As}_{1.00\pm 0.05}\text{S}_{0.9\pm 0.1}$
0.84	212	207	128	94	$\text{Fe}_{1.00}\text{As}_{1.00\pm 0.05}\text{S}_{1.0\pm 0.1}$
	179	177	115	81	$\text{Fe}_{1.00}\text{As}_{1.00\pm 0.05}\text{S}_{1.0\pm 0.1}$
0.94	219	210	130	84	$\text{Fe}_{1.00}\text{As}_{1.00\pm 0.05}\text{S}_{1.0\pm 0.1}$
	222	215	135	87	$\text{Fe}_{1.00}\text{As}_{1.00\pm 0.05}\text{S}_{1.0\pm 0.1}$

In Table 2, the sulfur ratio of 0.9 ± 0.1 at 0.74 V is lower than the value of 1.0 ± 0.1 at 0.84 and 0.94 V. Within the experimental uncertainties, it is impossible to establish if this difference is real and the simplest conclusion is that the oxidation of arsenopyrite is congruent for each element, even though the specimen is arsenic deficient.

The 1:1:1 oxidation stoichiometry is confirmed during the reaction since graphs of cumulative dissolved arsenic or cumulative dissolved sulfur versus cumulative dissolved iron are linear. There is no variation in the product ratios during the reaction at different potentials, shown for dissolved sulfur in Fig. 1(a). The slopes of best fit produce values of 1.0 and 0.60, respectively, for the ratio As:Fe and S(dissolved):Fe at each potential in good agreement with Table 2. Plots of cumulative charge against cumulative dissolved iron were also linear at each potential with values of $8.4\text{--}9.0e^-$ per mol Fe for the range 0.74–0.94 V.

As the stoichiometry was unaffected by potential at 25 °C, the reaction was only investigated at 0.84 V to check the influence of temperature, summarized in Table 3. The stoichiometry is 1:1:1 with respect to iron, arsenic and sulfur within the analytical error.

The oxidation stoichiometry is constant during the reaction since graphs of cumulative dissolved arsenic and cumulative dissolved sulfur against cumulative dissolved iron were linear during the reaction interval. Figure 1(b) shows this result for dissolved sulfur. The different symbols in the graph represent different electrodes and confirm the good reproducibility of the results. The slope of best fit produced values of 1.0 and 0.40, respectively, for As:Fe and S(dissolved):Fe, in good agreement with Table 3. The slope of the linear graph of cumulative charge versus cumulative dissolved iron was $7.5e^-$ per mol Fe at 75 °C.

The effect of mineral composition on the oxidation stoichiometry was checked at 25 °C. Stoichiometric arsenopyrite had a small surface area ($\sim 0.02\text{ cm}^2$)

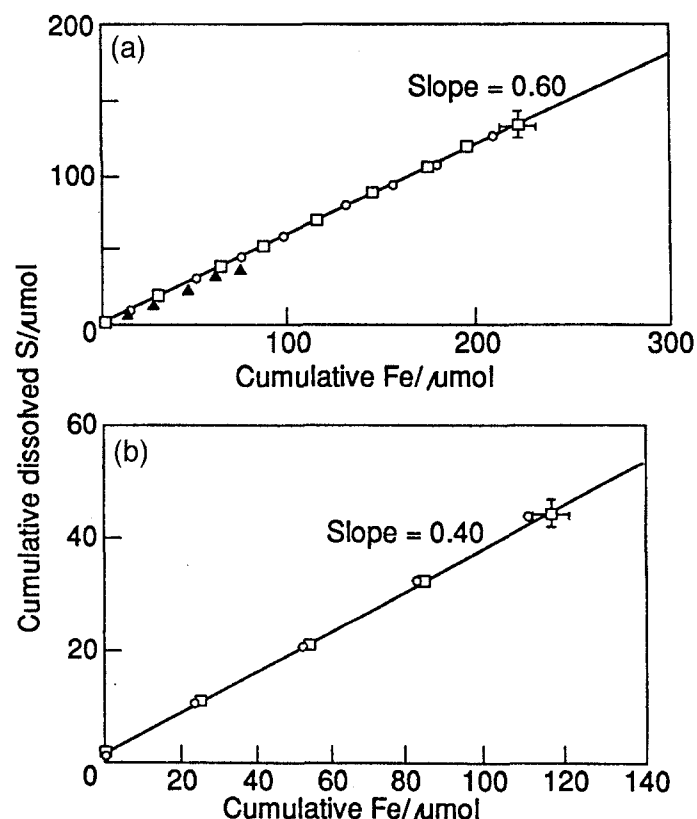


Fig. 1. Graph of dissolved sulfur against dissolved iron: for arsenic deficient arsenopyrite ($\text{FeAs}_{0.92}\text{S}$) (a) at \blacktriangle 0.74, \circ 0.84 and \square 0.94 V vs SHE and 25 °C; (b) at 0.84 V vs SHE and 75 °C. Bars on selected points show the uncertainty in the data. The different symbols at 75 °C show the reproducibility obtained with two different electrodes.

Table 3. Oxidation stoichiometry of arsenic deficient arsenopyrite ($\text{FeAs}_{0.92}\text{S}$) at 75°C , 0.84 V vs SHE, in 0.01 M KCl at pH 2. Repeated test used a different electrode

Total dissolved Fe / μmol	Total dissolved As / μmol	Total dissolved S / μmol	Total elemental S / μmol	Oxidation stoichiometry
112	108	44	78	$\text{Fe}_{1.00}\text{As}_{1.00\pm 0.05}\text{S}_{1.1\pm 0.1}$
117	114	44	72	$\text{Fe}_{1.00}\text{As}_{1.00\pm 0.05}\text{S}_{1.1\pm 0.1}$

and the most comprehensive data were collected at 0.94 V as shown in Fig. 2. The graphs confirm congruent dissolution of Fe and As and show that 9.1 e^- are produced per mol FeAsS oxidized. The dissolved sulfur ratio was 0.49, in close agreement with the data for arsenic deficient arsenopyrite. S was identified on the electrode surface by SEM/EDX and XRD but the yield was below the detection limit (0.2 mg) for all conditions. At 0.74 V , measurement of dissolved S was imprecise but the 1:1 relationship for dissolved Fe and As was confirmed. The totality of the data therefore indicates that the oxidation stoichiometry of arsenopyrite is not dependent on mineral composition.

At the end of an experiment, an amorphous, yellowish material containing iron and arsenic (identified by SEM/EDX) was observed on the electrode surface in addition to elemental sulfur. This material amounted to less than 4% of total Fe or As and was not investigated further. Similarly, an unidentified dark surface phase was observed in the initial stages

of oxidation at 0.74 V but the colour disappeared with progress of the reaction.

In summary, at 25°C and 75°C the dissolution stoichiometry of arsenopyrite is 1:1:1 for Fe:As:S, irrespective of bulk composition. The coulometric requirement at 25°C was $\sim 9\text{ e}^-$ per mol Fe, and at 75°C the requirement was 7.5 e^- per mol Fe. The stoichiometric dissolution of iron and arsenic agrees with acidic pressure oxidation of arsenopyrite in sulfuric acid between $130\text{--}180^\circ\text{C}$ [14]. However, for nonstoichiometric arsenopyrite the residual phase will eventually have a changed composition which must increasingly influence the oxidation process as the solid dissolves.

3.2. Speciation pattern

The speciation of the oxidation products was determined as follows. The amount of arsenopyrite oxidized during a run was calculated from the charge and the coulometric requirement (e.g., as in Fig. 2(c)). The measured concentration of each species was expressed as a fraction of the total mol of arsenopyrite oxidized at that stage of the reaction. The speciation was constant within each run, as expected from the linearity of plots such as Figs 1 and 2. Figure 3 shows the results for sulfur speciation for the oxidation of arsenic deficient arsenopyrite as a typical example. Table 4 gives a summary of all results as follows: (a) arsenic deficient arsenopyrite: effect of potential at 25°C and of temperature (75°C) at 0.84 V and (b) stoichiometric arsenopyrite: at 25°C and 0.94 V .

Table 4 shows that more Fe(III) is produced as the potential is increased at 25°C and that this trend is reversed at 75°C , when Fe(II) is predominant. This result is unexpected as Fe(III) is the thermodynamically favoured reaction product above 0.8 V [14]. The result did not arise as an artefact from reduction of Fe(III) at the counter electrode, since iron levels in the counter electrode compartment were negligible. Perhaps Fe(III) can be reduced at 75°C by the species $\text{S}(x)$, which had a much reduced yield ~ 0 at 75°C (see further below)? However, our result agrees with [14] where $\text{Fe(II)} \sim 75\%$ of the total dissolved Fe in the pressure leaching of arsenopyrite above 120°C , prior to slow homogeneous oxidation to Fe(III) by dissolved oxygen; and a fully adequate rationale for the stability of Fe(II) at elevated temperatures is lacking.

As(III) and As(V) ratios are practically constant for all conditions. As(V) is the thermodynamically

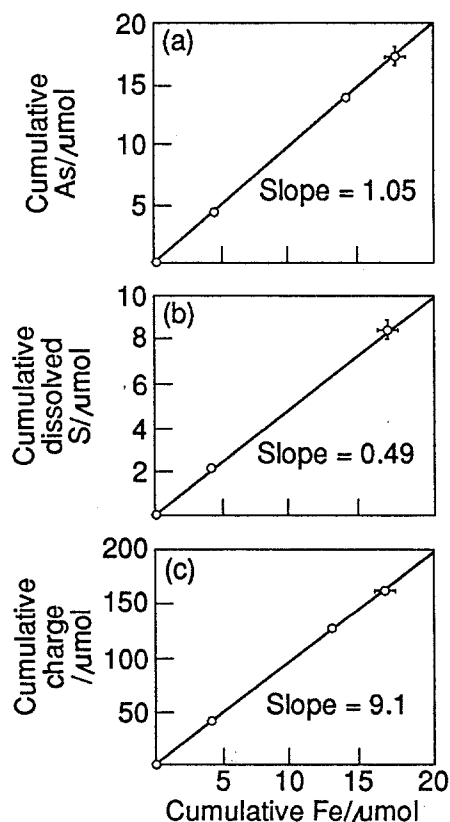


Fig. 2. Graph of (a) dissolved arsenic, (b) dissolved sulfur and (c) charge passed against dissolved iron at 0.94 V vs SHE and 25°C . Bars on selected points show the experimental uncertainty in the data.

Table 4. Distribution of iron, arsenic and sulfur oxidation products for arsenic deficient and stoichiometric arsenopyrite between 25–75 °C and 0.74–0.94 V vs SHE in 0.01 M KCl at pH 2

$FeAs_{0.92}S$		Mol of species/mol $FeAsS$ oxidized							
Temp. / °C	Potential / V vs SHE	Fe(II)	Fe(III)	As(III)	As(V)	S(VI)	S(x)	S	e^-
25	0.74	0.51	0.49	0.85	0.15	0.33	0.18	0.49	8.3
	0.84	0.20	0.80	0.85	0.15	0.33	0.28	0.39	9.0
	0.94	0.15	0.85	0.89	0.11	0.33	0.26	0.41	8.8
75	0.84	0.85	0.15	0.87	0.13	0.36	<0.02	0.62	7.5
$FeAsS$									
25	0.94	0.15	0.85	0.81	0.19	0.36	0.12	0.52	9.1

favoured reaction product but As(III) was found as the predominant species (~85%). As(V) was produced in the electrochemical oxidation of arsenopyrite in alkali [10–13] and in oxygen pressure leaching in acid [14]. By contrast, ferric-leaching [3, 28] and biooxidation [29] of arsenopyrite in acid produced As(III), although bacterial catalysis transforms As(III) to As(V) with time [29]. Tan and Dutrizac [30] found that dissolved As(III) was resistant to oxidation by Fe(III) in the presence of SO_4^{2-} but there was slow partial oxidation of As(III) to As(V) in SO_4^{2-} free chloride solution. This observation could imply that Fe(III) has reduced oxidizing power when present as an ion-pair with SO_4^{2-} (or HSO_4^-), but in the present work, synthetic mixtures of a typical test solution (80 ppm Fe(III), 80 ppm As(III), 13 ppm SO_4^{2-} in 0.01 M KCl at pH 2) in contact with a large Pt electrode held at 0.84 V failed to produce As(V) even after three days. Hence, As(III) oxidation is kinetically hindered and this

conclusion is consistent with claims that the oxidation of As(III) to As(V) is slow in the absence of catalysts [29, 31, 32].

Figure 3 shows that the distribution of sulfur products is constant during the reaction at each potential within analytical error. The S(VI) ratios are the same, irrespective of potential. The S(x) and S(0) ratios at 0.74 V appear to be different compared to those at 0.84 or 0.94 V. The S(x) ratio is at least $\pm 10\%$ uncertain and the difference is not significant. The S(0) ratio has an uncertainty of at least 15% which practically accounts for the deviation at 0.74 V. The alternative is to suppose that S(0) is oxidized to S(x) at the higher potentials but this is unlikely because S(0) is known to be stable at potentials up to 1.7 V [33]. Therefore, at 25 °C, S(VI), S(x) and S(0) are produced essentially in equimolar amounts at each potential. Table 4 shows that at 75 °C the S(VI) ratio is the same as at 25 °C. However, practically no S(x) is formed and

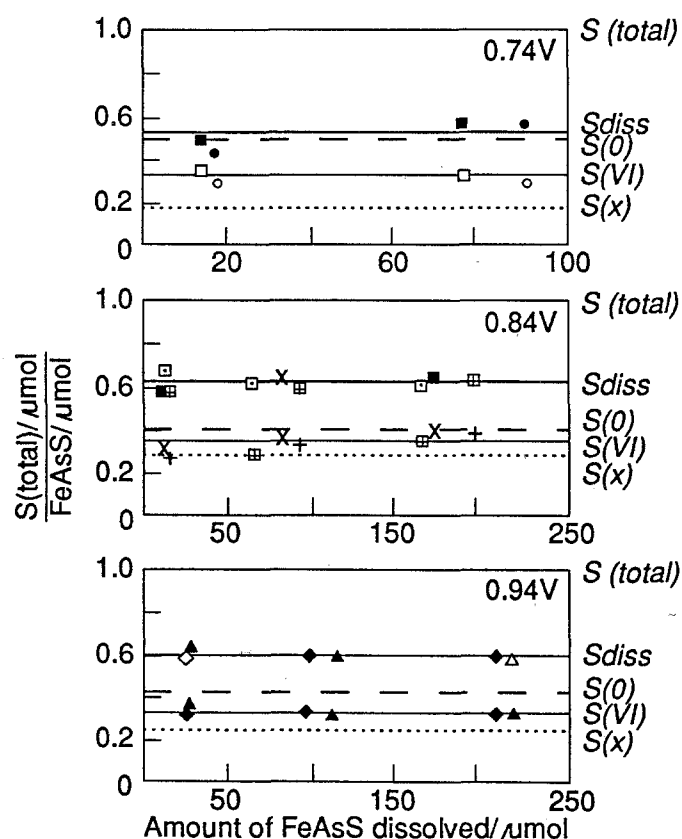


Fig. 3. Distribution of sulfur oxidation products at different potentials (vs SHE) and 25 °C for arsenic deficient arsenopyrite ($FeAs_{0.92}S$). Different symbols used at each potential represent data obtained using different electrodes. S(x) is the value $S_{diss} - S(VI)$. S is the value $1 - S_{diss}$. S_{diss} was measured by ICP-AES and S(VI) was measured by IC.

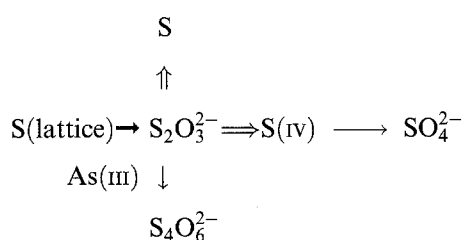
S(0) ratio is markedly greater. Table 4 indicates that stoichiometric arsenopyrite also produces the three sulfur oxidation products. S(vi) production is unchanged but different amounts of S(x) and S(0) appear to be formed. The analysis uncertainty for stoichiometric arsenopyrite is considerable because only small quantities could be dissolved from these samples in a reasonable time (surface area $\sim 0.02 \text{ cm}^2$). Therefore, the small difference between the S(x) and S(0) ratio for stoichiometric and arsenic deficient arsenopyrite in Table 4 is probably unreal, consistent with the result that the coulometric requirement for the two samples at 0.94 V is practically the same.

Attempts were made to identify the species S(x). x can be calculated from the ratios of Fe(II), Fe(III), As(III), As(V), S(vi) and S(0) at each potential, but this calculation has a very large uncertainty when the experimental errors are considered. For example, for 0.94 V and 25 °C, $x = 3 \pm 5$. This large uncertainty is similar for all conditions [27] and it is difficult to draw a conclusion. The only alternative was to identify sulfur species that are stable in acid, for example, dithionate, $\text{S}_2\text{O}_6^{2-}$; tetrathionate, $\text{S}_4\text{O}_6^{2-}$ and pentathionate, $\text{S}_5\text{O}_6^{2-}$ [34, 35] as candidates for S(x), without further resolution possible from the present data.

3.3. Reaction scheme

Thiosulfate is a key surface intermediate in the oxidation of sulfides (e.g., [18, 25]). In acid, thiosulfate can decompose to S and sulfite and also [34] form into polythionate (general formula $\text{S}_n\text{O}_6^{2-}$) in the presence of As(III). This reaction was demonstrated in cold HCl suggesting that high temperature inhibits the reaction. Polythionate form via an As-thiosulfate complex [37], although this mechanism has not been proven.

This background literature can be brought to account qualitatively for the sulfur speciation found in this work. If thiosulfate is presumed to be the initial S-based oxidation product formed on the arsenopyrite surface, it could interact with As(III) at the mineral surface to facilitate a pathway for the formation of polythionate. This reaction seems to be inhibited at high temperatures, which provides another rationale for our result that practically no S(x) was formed at 75 °C. Thiosulfate decomposition in acid would account for the presence of S and the sulfite decomposition product will oxidize rapidly to SO_4^{2-} at 0.7–0.9 V [18, 25]. This scheme for the S pathway in the oxidation of arsenopyrite is illustrated below (taking the polythionate $\text{S}(x) = \text{S}_4\text{O}_6^{2-}$):



The scheme limits the production of S to 50% of the total, consistent with most of the data in Table 4; but it also implies that inhibition of the path to S(x) at 75 °C would be reflected by an equal increase in the yields of both S and SO_4^{2-} . This prediction is not borne out for the results at 75 °C in Table 4, although the data is close, given the experimental uncertainties involved. Clearly, the proposed scheme is not proven and a future test would be measurement of sulfur speciation for the oxidation of arsenopyrite in the presence of cations which stabilize thiosulfate as a complex. Furthermore, *in situ* Raman identification of the surface sulfur species [38] on the arsenopyrite surface during oxidation would be revealing.

4. Conclusion

The oxidation of one mol of arsenopyrite produces one mol of Fe, As and S in acidic chloride solutions. This stoichiometry is unchanged by potential, temperature or bulk composition for arsenopyrite minerals. At 25 °C, Fe(II), Fe(III), As(III), As(V), S, SO_4^{2-} , S(x) (probably a polythionate: e.g., $\text{S}_4\text{O}_6^{2-}$) and $\sim 9e^-$ were produced per mol of arsenopyrite oxidized. At 75 °C, similar oxidation products but practically no S(x) were found; and $7.5e^-$ were produced per mol of arsenopyrite oxidized. A reaction scheme involving a thiosulfate intermediate has been postulated to account for the formation of the different sulfur products.

Acknowledgements

Jeff Dunn, Ann Howe and Harold Hughes helped with this study. Joanne Slattery typed the manuscript. The work was supported in part by a CSIRO–Curtin University–Industry scholarship and by the A. J. Parker Cooperative Research Centre for Hydro-metallurgy.

References

- [1] P. G. Fernandez, H. G. Linge and M. W. Wadsley, *J. Appl. Electrochem.* **26** (1996) 575.
- [2] S. R. La Brooy, H. G. Linge and G. S. Walker, *Minerals Engineering* **7** (1994) 1213.
- [3] H. G. Linge and W. G. Jones, *ibid.* **6** (1993) 873.
- [4] G. M. Kostina and A. S. Chernyak, *J. Appl. Chem. USSR* **49** (1976) 1566.
- [5] *Idem, ibid.* **50** (1977) 2571.
- [6] *Idem, ibid.* **52** (1979) 1457.
- [7] M. J. V. Beattie and G. W. Poling, *Int. J. Miner. Process.* **20** (1987) 87.
- [8] A. N. Buckley and G. W. Walker, *Appl. Surf. Sci.* **35** (1988/89) 227.
- [9] P. Bhakta, J. W. Langhans and K. P. V. Lei, Report of Investigation RI 9258, US Bureau of Mines (1989).
- [10] J. B. Hiskey and V. Sanchez, in 'Arsenic Metallurgy Fundamentals and Application', TMS–AIME, Warrendale, PA (1988) p. 59.
- [11] V. Sanchez and J. B. Hiskey, *Met. Trans. B* **19** (1988) 943.
- [12] V. Sanchez and J. B. Hiskey, in 'Electrochemistry in Mineral and Metal Processing', vol 2, Electrochemical Society, NJ, (1988) p. 264.
- [13] V. Sanchez and J. B. Hiskey, *Miner. & Metall. Process.* **8** (1991) 1.

- [14] V. G. Papangelakis and G. P. Demopoulos, *Can. Met. Quart.* **29** (1990) 1.
- [15] *Idem, ibid.* **29** (1990) 13.
- [16] J. T. Woodcock, *Proc. Aus. I.M.M.* **198** (1961) 47.
- [17] H. G. Linge, *Hydrometallurgy* **2** (1976) 51.
- [18] R. E. Meyer, *J. Electroanal. Chem. Interfac. Electrochem* **101** (1979) 59.
- [19] R. T. Lowson, *Chem. Rev.* **82** (1982) 461.
- [20] E. Peters and F. M. Doyle, in 'Challenges in Mineral Processing', SME, Littleton, (1989) chapter 31.
- [21] J. Dutrizac, *Hydrometallurgy* **29** (1992) 1.
- [22] B. J. Reedy, J. K. Beattie and R. T. Lowson, *Spectrochimica Acta* **46A** (1990) 1513.
- [23] G. W. Walker, P. E. Richardson and A. N. Buckley, *Int. J. Mineral Processing* **25** (1989) 153.
- [24] F. K. Crundwell, *Hydrometallurgy* **21** (1988) 155.
- [25] K. Osseo-Asare, *ibid.* **29** (1992) 61.
- [26] R. T. Shuey, 'Semiconducting Ore Minerals', Elsevier Scientific, Amsterdam (1975).
- [27] P. G. Fernandez, PhD thesis, Curtin University of Technology, Perth (1992).
- [28] J. Barrett, M. N. Hughes and A. Russell, in 'Randol Gold Forum Square Valley '90', Randol International, Golden, Co. (1990) p. 135.
- [29] J. Barrett, M. N. Hughes, G. I. Karavaiko and P. A. Spencer, 'Metal Extraction by Bacterial Oxidation of Minerals', Ellis Horwood, London (1993).
- [30] L. K. Tan and J. E. Dutrizac, *Anal. Chem.* **57** (1985) 1027; **57** (1985) 2615.
- [31] W. H. Kao and T. Kuwana, *J. Electroanal. Chem. Interfac. Electrochem.* **169** (1984) 167; **193** (1985) 145.
- [32] J. S. Yates and H. C. Thomas, *J.A.C.S.* **78** (1956) 3950.
- [33] E. Najdeker and E. Bishop, *J. Electroanal. Chem. Interfac. Electrochem.* **41** (1973) 79.
- [34] D. M. Yost and H. Russell Jr., in 'Systematic Inorganic Chemistry of the Fifth and Sixth Group Nonmetallic Elements', Prentice Hall, New York (1944) p. 387.
- [35] D. Lyons and G. Nickless, in 'Inorganic Sulphur Chemistry', Elsevier Scientific Amsterdam (1968) p. 509.
- [36] F. A. Cotton and G. Wilkinson, 'Advanced Inorganic Chemistry - A Comprehensive Text', Wiley Eastern, New Delhi (1985).
- [37] R. K. Eremenko and A. I. Brodsky, *J. Gen. Chem. USSR* **25** (1955) 1189.
- [38] P. D. Harvey and I. S. Butler, *J. Raman Spectrosc.* **17** (1986) 329.